3D Jet Tomography and the Twisted Color Glass Condensate

A. Adil[a], M. Gyulassy[a], T. Hirano[a]. *

[a]Columbia University, Department of Physics, 538 West 120-th Street, New York, NY 10027

Jet Tomography is proposed as a new test of Color Glass Condensate (CGC) initial conditions in non-central $A+A$ collisions. The k_T factorized CGC formalism is used to calculate the rapidity twist [1]. A new observable, ΔR_{AA} is proposed to test a novel high p_T rapidity twist predicted by the CGC model. Extensions to $v_1(p_T,\eta)$ are in [2].

1. Introduction:

It was pointed out in Ref.[1] that the QCD matter produced in noncentral $A+A$ nuclear reactions violates boost invariance in the transverse plane. At RHIC and LHC it may be large enough to be observable via 3D $(p_\perp,\phi,\eta)$ extensions[1] of jet tomography[3]. These trapezoidal features are well reproduced by gluon saturation models such as in the Kharzeev-Levin-Nardi (KLN)[4] implementation of the Color Glass Condenstate (CGC) theory[5,6] .

The strongest support for the KLN/CGC approach is its ability to reproduce the systematics of the energy and nuclear size dependence of the global p_T integrated dN_{ch}/dy. This results from a specific dependence of the saturation scale, Q_s, on $\sqrt{s}$ and A. Both experimental and theoretical control over the initial conditions in $A+A$ at RHIC are essential to strengthen the current case for the discovery of new forms of matter, the strongly coupled Quark Gluon Plasma (sQGP) and CGC, at RHIC [8–10].

The CGC model produces approximately the same rapidity twist of the bulk as the model used in [1]. At higher p_T the CGC predicts even greater rapidity twist away from the beam axis than the bulk as illustrated in Fig.1. This anomalous rapidity twist effect is opposite to that discussed in [1]. It occurs because the different nuclei are probed at asymmetric Bjorken momentum fractions while producing high p_T matter.

2. The Local Gluon Distribution:

The local generalization of the GLR formula[7] used by KLN[4] and Hirano and Nara [12] is given by

$$\frac{dN_g}{dp_T d^2x_T d\eta} = \frac{4\pi}{C_F}\frac{\alpha_s(p_T^2)}{p_T}\int^{p_T} d^2k_T \phi_A(x_1,(\frac{\vec{k}_T+\vec{p}_T}{2})^2;\vec{x}_T)\phi_B(x_2,(\frac{\vec{k}_T-\vec{p}_T}{2})^2;\vec{x}_T). \quad (1)$$

*This work was partially supported by the United States Department of Energy under Grants No. DE-FG02-93ER40764

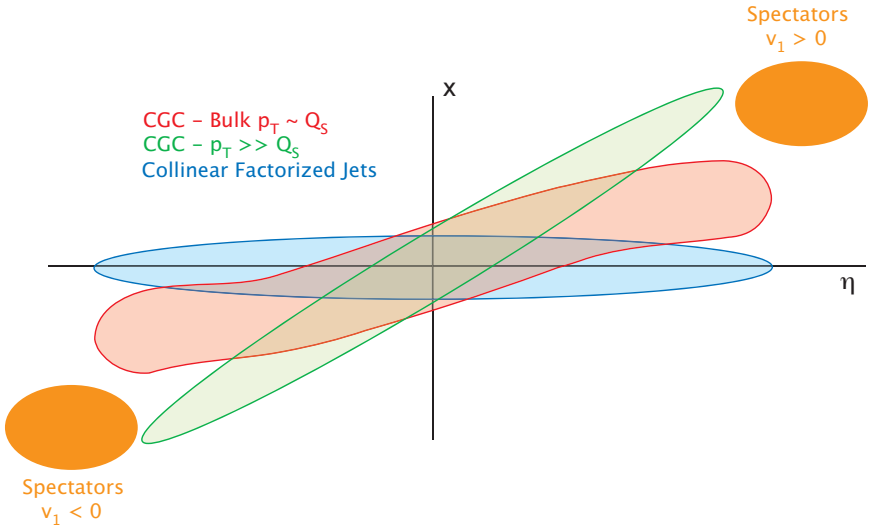

Figure 1. Illustration of the initially twisted sQGP gluon density[1] relative to the beam axis in the (x, η) reaction plane. Also shown are the relative rotations of the high $p_T \gg Q_s$ jet partons in the k_T factorized CGC model as well as conventional collinear factored pQCD. The projectile and spectator nuclei are indicated by half circles together with the sign convention of low p_T directed flow v_1.

$C_F = \frac{N_C^2-1}{2N_C}$ and the collinear momentum fractions are given by kinematics, $x_{1,2} = p_T \exp(\pm\eta)/\sqrt{s}$. The QCD coupling, α_s, is evaluated at p_T^2 and regulated at low p_T by imposing $\alpha_{\rm max} = 0.5$.

$\phi_{A,B}$ are the unintegrated gluon distributions which, in principle, possess a Bjorken x dependence determined by nonlinear evolution equations of the CGC theory[5,6] and their k_T dependence is fixed by a characteristic saturation momentum, $Q_s(x)$. We use the following Lorentzian form of The KLN model $\phi_{A,B}$ for all values of k_T.

$$\phi_A(x, \vec{k}_T; \vec{x}_T) = \frac{\kappa}{\alpha_s(Q_{s,A}^2)} \frac{Q_{s,A}^2}{k_T^2 + Q_{s,A}^2 + \Lambda^2}. \tag{2}$$

The momentum scale $\Lambda = 0.2$ GeV is a regulator for the high rapidity $y > 4.5$ region as in [12]. The constant $\kappa \sim 0.5$ is a parameter set to reproduce $dN_g/d\eta \sim 1000$ at midrapidity central collisions. The transverse coordinate dependence is implicit in the saturation momentum determined numerically for each nucleus.

$$Q_{s,A}^2(x, \vec{x}_T) = \frac{2\pi^2}{C_F} \alpha_s(Q_{s,A}^2) x G_{\rm nuc}(x, Q_{s,A}^2) T_A(\vec{x}_T), \tag{3}$$

where T_A is the Glauber profile of nucleus A. We use standard diffuse Woods-Saxon profiles.

The KLN parametrization is used for the nucleonic gluon distribution.

$$x G_{\rm nuc}(x, Q^2) = K \log\left(\frac{Q^2 + \Lambda^2}{\Lambda_{QCD}^2}\right) x^{-\lambda} (1-x)^n \tag{4}$$

The momentum scales Λ and $\Lambda_{\rm QCD}$ are set to 0.2 GeV. As in the KLN approach, we set $\lambda = 0.2$ and $n = 4$. $K \sim 1.35$ is used to set $\langle Q_s^2(x = 0.01)\rangle \sim 2$ GeV^2 for central collisions at midrapidity.

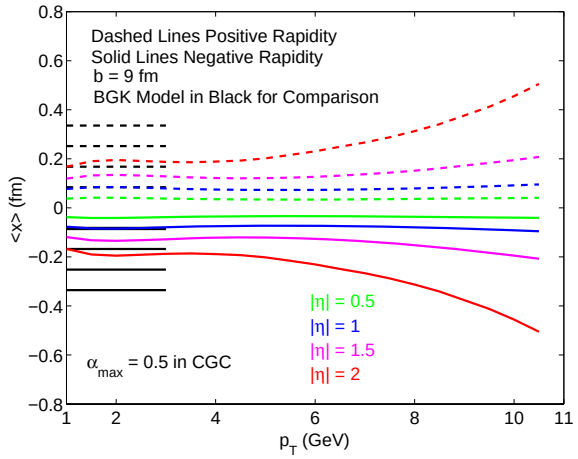

Figure 2. Average transverse spatial coordinate $\langle x\rangle$ for produced gluonic matter as in [1] as well as in the current CGC model.

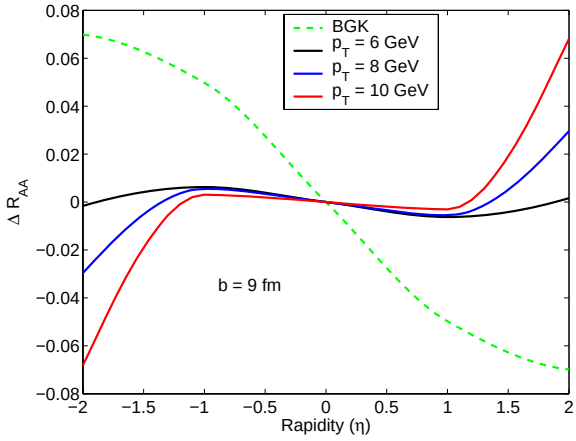

Figure 3. ΔR_{AA} as a function of η for different p_T at $b = 9$ fm.

We measure the shift of material away from the centre of the reaction plane by calculating the average horizontal transverse coordinate.

$$\langle x\rangle(p_T,\eta) = (\int d^2x_T x \frac{dN_g}{dp_T d^2x_T d\eta})/(\int d^2x_T \frac{dN_g}{dp_T d^2x_T d\eta}) \tag{5}$$

Fig. 2 shows $\langle x\rangle$ as a function of p_T and η for the model used in [1] as well as for the current CGC model (for $b = 9$ fm). The rapidity twist of the BGK model is seen by the increasing $\langle x\rangle$ as η increases for the bulk $p_T \leq 3$ GeV matter. While the bulk $\langle x\rangle$ of the CGC model is similar to the bulk BGK shifts, the high p_T shifts behave oppositely. We show in Fig. 2 that the rapidity twist $(d\langle x\rangle/d\eta)$ increases at high $p_T > 6$ GeV.

3. Tomography and the Inverse Twist:

The nuclear modification factor, R_{AA}, measures the deviation of the produced nucleus-nucleus spectrum, if any, from a simple binary scaled p-p spectrum. The twist effect investigated in the previous section can be observed by looking at the $R_{AA}(p_T,\eta,\phi)$ of jets in the transverse plane. The azimuthal dependence of R_{AA} will change as a function of η for a given p_T jet due to the differing twist of the jet distribution over η. We use the geometric model in [13] where the nuclear modification factor is obtained by,

$$R_{AA}(p_T,\eta,\phi) = (\int d^2x_T e^{-\mu\chi(\vec{x}_T,\phi,\eta)} \frac{dN_g}{dp_T d^2x_T d\eta}(p_T,\eta))/(\int d^2x_T \frac{dN_g}{dp_T d^2x_T d\eta}(p_T,\eta)). \tag{6}$$

$\mu = 0.04$ is the parameter used to set $R_{AA}(\eta = 0, b = 0) \sim 0.25$. Opacity, χ, is the line integral over the bulk distribution that is the cause of the attenuation experienced by the jet, calculated as in [13]. The length dependence of opacity is characteristic of radiative parton energy loss in Bjorken expanding matter.

The anti-twist effect can most easily be observed via the observable $\Delta R_{AA}(p_T, \eta) = R_{AA}(p_T, \eta, \phi = 0) - R_{AA}(p_T, \eta, \phi = \pi)$. Fig. 3 shows ΔR_{AA} as a function of η for different values of the p_T. Note that for all p_T values there exists a rapidity at which the ΔR_{AA} flips sign. The change in sign is a novel prediction using the KLN/CGC model. In conventional factorized QCD jet production, the high p_T one does not see this sign change. The extension to directed flow, v_1, is achieved in [2].

REFERENCES

1. A. Adil, M. Gyulassy, arXiv:nucl-th/0505004
2. A. Adil, M. Gyulassy, T. Hirano, Phys. Rev. C **72**, 034907 (2005). arXiv:nucl-th/0509064
3. M. Gyulassy, I. Vitev, X. N. Wang and B. W. Zhang, arXiv:nucl-th/0302077. in "Quark Gluon Plasma 3", (editors: R.C. Hwa and X.N. Wang, World Scientific, Singapore.) p. 123-191; P. Jacobs and X. N. Wang, Prog. Part. Nucl. Phys. **54**, 443 (2005) [arXiv:hep-ph/0405125].
4. D. Kharzeev, E. Levin and M. Nardi, Nucl. Phys. A **730**, 448 (2004) [Erratum-ibid. A **743**, 329 (2004)] [arXiv:hep-ph/0212316]; Nucl. Phys. A **747**, 609 (2005) [arXiv:hep-ph/0408050].
5. E. Iancu, A. Leonidov and L. D. McLerran, Nucl. Phys. A **692**, 583 (2001) [arXiv:hep-ph/0011241].
6. J. P. Blaizot and F. Gelis, Nucl. Phys. A **750**, 148 (2005) [arXiv:hep-ph/0405305].
7. L. V. Gribov, E. M. Levin and M. G. Ryskin, Phys. Rept. **100**, 1 (1983); Phys. Lett. B **100**, 173 (1981); E Laenen and E. M. Levin, Ann. Rev. Nucl. Part. Sci. **44**, 199 (1994).
8. M. Gyulassy and L. McLerran, Nucl. Phys. A **750**, 30 (2005) [arXiv:nucl-th/0405013]; See also articles by T.D.Lee, J.P. Blaizot, B. Muller, E. Shuryak, H. Stöcker, X.N. Wang, Nucl. Phys. A **750** (2005), pp.1-171.
9. K. Adcox *et al.* [PHENIX Collab.], Nucl. Phys. A, **757** pp 184-283 (2005); B. B. Back *et al.* [PHOBOS Collab.], Nucl. Phys. A **757** pp 28-101 (2005); I. Arsene *et al.* [BRAHMS Collab.], Nucl. Phys. A **757** pp 1-27 (2005); J. Adams *et al.* [STAR Collab.], Nucl. Phys. A **757** pp 102-183 (2005);
10. T. Hirano and M. Gyulassy, [arXiv:nucl-th/0506049]
11. D. Kharzeev and M. Nardi, Phys. Lett. B **507**, 121 (2001); D. Kharzeev and E. Levin, *ibid.* B, **523**, 79 (2001); D. Kharzeev, E. Levin and M. Nardi, [arXiv:hep-ph/0111315]; D. Kharzeev, E. Levin and M. Nardi, Nucl. Phys. A, **730**, 448 (2004).
12. T. Hirano and Y. Nara, Nucl. Phys. A **743**, 305 (2004) [arXiv:nucl-th/0404039].
13. A. Drees, H. Feng and J. Jia, arXiv:nucl-th/0310044.